ACS APPLIED MATERIALS & INTERFACES

Research Article

www.acsami.org

Enhanced Proliferation and Osteogenic Differentiation of Mesenchymal Stem Cells on Graphene Oxide-Incorporated Electrospun Poly(lactic-*co*-glycolic acid) Nanofibrous Mats

Yu Luo,[†,‡,⊥] He Shen,[†,⊥] Yongxiang Fang,[§,∥] Yuhua Cao,[†] Jie Huang,[†] Mengxin Zhang,[†] Jianwu Dai,*[,†,§] Xiangyang Shi,*[,‡] and Zhijun Zhang*[,†]

[†]Key Laboratory of Nano-Bio Interface, Division of Nanobiomedicine, Suzhou Institute of Nano-Tech and Nano-Bionics, Chinese Academy of Sciences (CAS), 398 Ruoshui Road, Suzhou 215123, China

[‡]College of Chemistry, Chemical Engineering and Biotechnology, Donghua University, Shanghai 201620, China

[§]State Key Laboratory of Molecular Developmental Biology, Institute of Genetics and Developmental Biology, Chinese Academy of Sciences (CAS), Beijing 100190, China

[∥]State Key Laboratory of Veterinary Etiological Biology, Key Laboratory of Veterinary Public Health of Agricultural Ministry, Lanzhou Veterinary Research Institute, Chinese Academy of Agricultural Sciences, Lanzhou 730046, China

Supporting Information

ABSTRACT: Currently, combining biomaterial scaffolds with living stem cells for tissue regeneration is a main approach for tissue engineering. Mesenchymal stem cells (MSCs) are promising candidates for musculoskeletal tissue repair through differentiating into specific tissues, such as bone, muscle, and cartilage. Thus, successfully directing the fate of MSCs through factors and inducers would improve regeneration efficiency. Here, we report the fabrication of graphene oxide (GO)-doped poly(lactic-*co*-glycolic acid) (PLGA) nanofiber scaffolds via electrospinning technique for the enhancement of osteogenic differentiation of MSCs. GO-PLGA nanofibrous mats with three-dimensional porous structure and smooth surface can be readily produced via an electrospinning technique. GO plays two roles in the nanofibrous mats: first, it enhances the hydrophilic performance, and protein- and inducer-adsorption ability of the nanofibers. Second, the incorporated GO accelerates the human MSCs (hMSCs) adhesion and proliferation versus pure PLGA nanofiber and induces the osteogenic differentiation. The incorporating GO scaffold materials may find applications in tissue engineering and other fields.

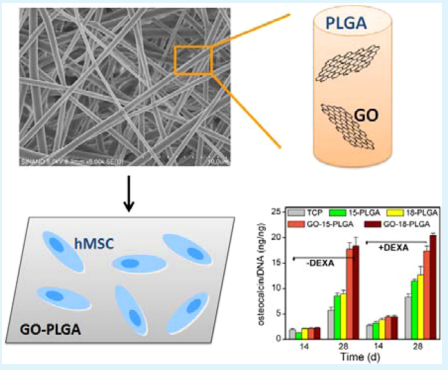

KEYWORDS: *nanofibrous mat, electrospinning, graphene oxide, mesenchymal stem cells, osteogenic differentiation, tissue engineering*

INTRODUCTION

Nanofibers consisting of different components are generally considered as composite nanofibers, which endow the fibers with desired functionalities.[1,2] For example, Xiao et al. reported that poly(acrylic acid)−poly(vinyl alcohol) (PVA) nanofibers mingled with iron nanoparticles show superior environmental remediation capability.[3] Additionally, gold or palladium nanoparticles-immobilized polyethylenimine−PVA nanofibers can be explored as efficient and reusable catalysts.[4,5] Inorganic nanotubes, such as multiwalled carbon nanotubes-, halloysite nanotubes-, or synthetic silicate clay material-doped poly(lactic-*co*-glycolic acid) (PLGA) nanofibers, have been developed for loading and sustained release of drugs.[6−8] Similarly, hybrid nanofibers have been applied for tissue engineering. Meng et al. found that superparamagnetic responsive nanofibrous scaffolds under static magnetic field could enhance the osteogenesis for bone repair in vivo.[9] However, how to efficiently accelerate growth and differentiation still remain great challenges. Fabrication of suitable bioactive scaffolds that can mimic the extracellular matrices (ECM) is an essential prerequisite for tissue engineering applications.[10−14]

Electrospinning is a simple and versatile technique used to fabricate fibers with a diameter ranging from tens of nanometers to a few micrometers.[15] The diameter of fibers is similar to the type I collagen, a major insoluble fibrous protein in the ECM. Additionally, the three-dimensional (3D) porous netlike structure of nanofibrous mat can well mimic the natural ECM,[16−19] making electrospun nanofibers ideal substrates for cell attachment and proliferation.[20]

PLGA with excellent biocompatibility and biodegradability has been widely used to form electrospun nanofibers and applied for tissue engineering.[21−23] Soscia et al. reported that the micropatterned PLGA nanofiber craters could promote the differentiation and organization of salivary gland cells.[24] Haider

Received: January 29, 2015
Accepted: March 5, 2015
Published: March 5, 2015

DOI: 10.1021/acsami.5b00862
ACS Appl. Mater. Interfaces 2015, 7, 6331−6339

et al. observed that the formation of PLGA/hydroxyapatite nanorods (nHA) hybrid nanofiber scaffold could accelerate bone tissue regeneration, in which nHA were used as nanocarrier for grafting differentiating inducer (insulin).[25] Shi and co-workers prepared laponite (LAP)−PLGA nanofibers for human mesenchymal stem cells (hMSCs) culture. They found that the LAP-doped nanofibers could stimulate the osteogenic differentiation of hMSCs.[7] Caballero et al. fabricated the PLGA nanofibers to load the connective tissue growth factor. Their study showed that the formed nanofibers could regulate the elastogenesis in human umbilical cord-derived mesenchymal stem cells.[26]

Graphene oxide (GO), a novel one-atom-thick two-dimensional carbon material, with many unique physicochemical properties, such as large surface area, sp^2 carbon domains, and hydrophilic functional groups, has attracted much attention in the field of biomedicine in recent years.[27] Previous work has demonstrated that GO could efficiently bind aromatic anticancer drugs,[28,29] genes,[30,31] and proteins[32−34] through $\pi-\pi$ stacking, electrostatic interaction, and hydrophobic interaction. Utilizing the strong adsorption capacity of graphene and GO, Lee et al. reported that graphene and GO substrates could enrich the proliferation and differentiation agents on the surface of graphene and GO sheets. Therefore, graphene and GO substrates could accelerate the adhesion, growth and differentiation of MSCs.[35,36] Additionally, it had been reported that GO could facilitate the attachment, proliferation and osteogenic and myoblast differentiation of MSCs.[37,38]

Human MSCs isolated from umbilical cord are multipotential stem cells that have an inherent ability to differentiate into many kinds of lineages, for instance, osteogenic, chondrogenic, myogenic, adipogenic, and neurogenic lineages.[39] MSC is a very important part of tissue engineering, where cells are combined with artificial scaffold to regenerate tissues. By controlling the substrate properties and applying growth factor inducers, MSCs could be induced to differentiate into specific cell types for regenerative applications.[40,41]

Motivated by the versatile electrospinning approach for ECM mimicking nanofibrous mats fabrication and the unique properties of GO in adsorption of protein and regulation of MSCs differentiation, we prepared electrospun GO-incorporated PLGA nanofibrous mats to form novel scaffold materials for bone tissue engineering. In this study, GO-incorporated electrospun PLGA nanofibers were formed and characterized. After GO was doped into PLGA nanofibers, properties of the nanofibers, such as hydrophilic property and adsorption capacity, were changed. Our aim was to investigate the effects of GO-incorporated PLGA nanofibrous platforms on hMSCs metabolism, such as attachment, growth and differentiation. In culture medium with an osteogenic inducer, hMSCs seeded on nanofibrous substrates could be differentiated into osteoblasts. Alkaline phosphatase activity, osteocalcin secretion, and marker genes expression were tested to reveal the role of GO-doped PLGA nanofibrous scaffolds during hMSCs differentiation. Finally, the possible reasons for the effect of GO-incorporated PLGA nanofibrous mats on hMSCs differentiation were discussed.

EXPERIMENTAL SECTION

Materials. PLGA (molecular weight = 200 000, LA/GA = 50/50) was purchased from Jinan Daigang Bio-technology Co., Ltd. (China). GO was prepared by oxidation of graphite using a modified Hummers method.[42] MSCs originated from human umbilical cord were friendly provided by Nanjing Gulou Hospital (Nanjing, China). Dulbecco's modified Eagle's medium/F12 (DMEM/F12, 50/50) was purchased from Corning. Fetal bovine serum (FBS), penicillin, trypLE express, and streptomycin were purchased from Gibco (UK). Dexamethasone (DEXA), β-glycerophosphate (β-GP), ascorbic acid (AA), *p*-nitrophenyl phosphate, and *p*-nitrophenol standard were obtained from Sigma. The BCA protein assay kit was from Beyotime Institute Biotechnology Co., Ltd. (Shanghai, China). The Picogreen DNA quantification kit was from Molecular Probes, Inc. (Eugene, OR). All other chemicals with reagent grade were from Sinopharm Chemical Reagent Co., Ltd. (Shanghai, China). The water used in all the experiments was purified using a Milli-Q Plus 185 water purification system (Millipore, Bedford, MA).

Fabrication of GO-Incorporated Electrospun PLGA Nanofibers. A suspension of PLGA (15 wt %) mixed with 1% GO was prepared by dispersing 30 mg of GO into 20 mL of a tetrahydrofuran/dimethylformamide mixture solvent (3/1, v/v) with vigorous magnetic stirring to form a homogeneous solution. Then 3 g of PLGA was added into the above solution at 4 °C for 24 h, and the solution was sonicated for 10 min using a water bath ultrasonic cleaner (50 W), SK1200H, Shanghai KUDOS Inc., China) before use. The PLGA/GO suspension used for electrospinning was loaded into a syringe with a needle, and the feed rate was controlled by syringe pump at 1 mL/h. The high-voltage and other equipment supply (BGG40/2, Institute of Beijing High Voltage Technology, China) was connected to the needle by a high-voltage insulating wire with two clamps at the ends. An aluminum board was used as the collector connected to the ground. The electrospinning setup can be found in our previous report.[43] The distance of tip to collector was set as 20 cm, and the electrospinning voltage was kept at 10 kV. The temperature was kept at 20−25 °C, and the humidity was kept at 50%. The prepared nanofibrous mat was dried for 24 h at 37 °C to remove the trace solvent under vacuum.

Characterization. The morphology of nanofibrous mats was observed by scanning electron microscopy (SEM), according to the protocol described in a previous report.[44] The PLGA nanofibrous mats with and without GO doping were characterized by Fourier transform infrared (FTIR, Nicolet Nexus 670 FTIR spectrometer) and Raman (LABRAM HR spectrometer) spectroscopies at room temperature. The confocal microprobe Raman system is equipped with a holographic notch filter and a CCD detector. A long working distance 50× objective was used to collect the signal. The size of the laser spot is 1.7 mm. The mechanical properties of nanofibrous mats were tested by a material testing machine (H5K-S, Hounsfield, UK). All the PLGA nanofibrous mats were cut into small strips with the width × gauge length = 10 × 50 mm, and three strips from different sites of each fibrous mats sample were chosen for the tensile test. Stress and strain were calculated according to the literature.[7] The surface hydrophilicity of the PLGA and GO-incorporated PLGA nanofibrous mats was evaluated via a water contact angle measurement using a contact angle goniometer (DSA-30, Kruss, Germany).[7]

Protein and Inducer Preconcentrated Capacity of GO-Incorporated PLGA Nanofibrous Mats. DEXA, ascorbic acid, and protein adsorption onto the electrospun fibrous mats was measured using UV−vis spectroscopy. Briefly, the nanofibrous samples of PLGA or GO-incorporated PLGA were cut into 10 × 10 mm, fitted into a tube, soaked in 75% ethanol for 2 h, and then rinsed three times with phosphate buffered saline (PBS). The wetted scaffolds were exposed to BSA solution (3 mL, 4 mg/mL in PBS buffer) for 24 h in a vapor-bathing constant temperature vibrator at 37 °C. After incubation, the nanofibrous mats were taken out, and the concentration of the protein was measured according to the vendor's protocol.

Hemocompatibility. Blood from Sprague−Dawley rats was extracted and stabilized with heparin. Then red blood cells (RBCs) were obtained. Hemocompatibility test was carried out following the procedure stated in the literature.[45]

In Vitro Cell Culture: Cell Attachment and Proliferation. A small piece of human umbilical cord was harvested from a pregnant woman and kept in a sterilized centrifuge tube with 0.9% saline solution, then washed twice with PBS (added with 1% antibiotic−

DOI: 10.1021/acsami.5b00862
ACS Appl. Mater. Interfaces 2015, 7, 6331−6339

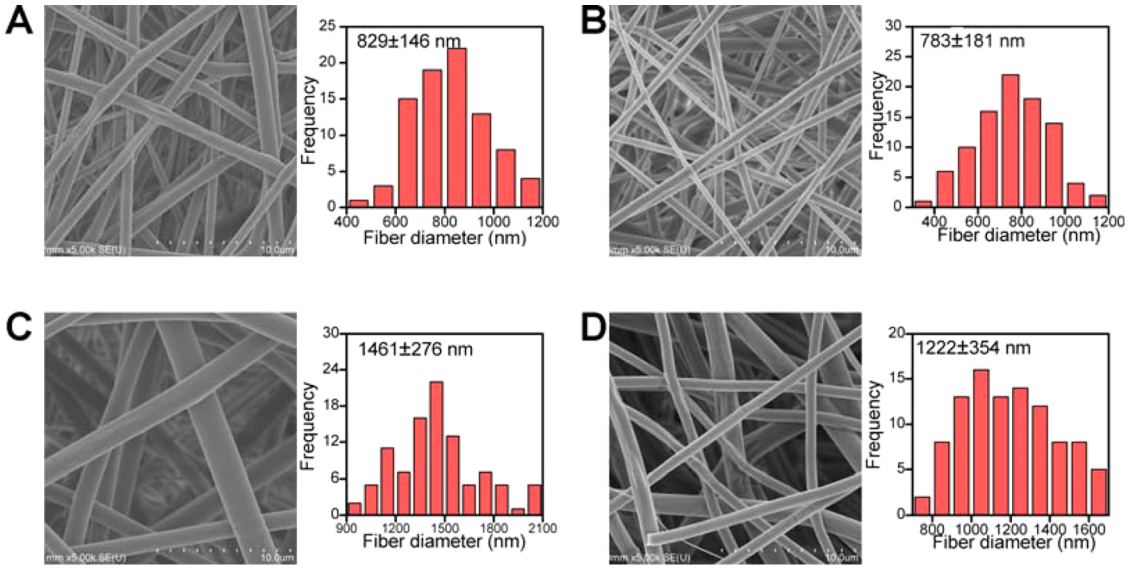

Figure 1. SEM images (left) and diameter distribution of nanofibers (right) of (A) 15-PLGA, (B) GO-15-PLGA, (C) 18-PLGA, and (D) GO-18-PLGA nanofibers, respectively (scale bar = 10 μm).

antimycotic) and transferred into cell culture dishes. The culture medium was changed every 3 days until the 80% confluence was reached. The cells were then passaged twice and frozen in liquid nitrogen. DMEM/F12 (50/50) supplemented with 10% FBS, 100 U/mL penicillin, and 100 μg/mL streptomycin solution was used throughout this process.

MTT assay was used to quantitatively evaluate the cell attachment and proliferation. Before cell seeding, PLGA and GO-incorporated PLGA nanofibers were sterilized with 75% alcohol for 2 h, followed by washing 3 times using PBS and soaking overnight in DMEM/F12 (50/50) containing 10% FBS. TCPs without materials were set as control. Then, hMSCs (passage 5) were seeded at a density of 2×10^4 and 1×10^4 cells per well (24-well plates, Corning Inc., Corning, NY) for the cell attachment and proliferation assay, respectively. Cell attachment and proliferation assays were performed according to our previous work.[44] Mean and standard deviation for the triplicate wells for each sample were reported.

Morphology of hMSCs Cultured on the Scaffolds. After being cultured for 28 d, the scaffolds with hMSCs were rinsed with PBS to remove nonadherent cells, and subsequently dehydrated according to the protocol described previously.[44] Dry samples were sputter coated with a 12 nm-thick gold film before SEM observation of the cell morphology.

RT-PCR for Marker Genes. To investigate the cell phenotype, mRNA was analyzed using real-time polymerase chain reaction (RT-PCR). After 14 and 28 d culture, the specimens were washed by PBS for three times, and then suspended in 1 mL of cold TRIzol Reagent (Life Technologies Co.). Total RNA of each sample was extracted using a standard TRIzol protocol, and resuspended in 50 μL of RNase-free water. The cDNA was generated using a transcriptase reaction mix (SuperScript III First-Strand Synthesis System, Life Technologies) as the protocol. The cDNA was stored at −20 °C until further analyses. Quantitative PCR analysis was performed in triplicate (n = 3) using a power SYBR green RT-PCR kit (Life Technologies) protocol. Glyceraldehyde-3-phosphate dehydrogenase (GAPDH) was used as an endogenous housekeeping gene to determine the other gene relative transcripts. Data were analyzed using a previously reported method and presented using the ΔΔCt method.[45] Cells grown on the TCP substrates were set as control, and the relative levels of marker genes expression were designed as one-fold. Primer sequences are available in Table S1 (Supporting Information). CD44 and CD105 are marker genes of hMSCs. Osteogenic marker genes are alkaline phosphatase (ALP), collagen type I (Col I), and osteocalcin (Ocn).

Alkaline Phosphatase Activity. For osteogenic differentiation, 1% β-GP solution, 1% ascorbic acid solution, and 10^{-7} M osteogenic inducer DEXA was added to cell culture medium. To investigate whether the GO-incorporated PLGA scaffolds stimulate the hMSC osteogenic differentiation or not, the cell culture medium without DEXA was set as control group. Then, to each sample was added Reporter Lysis Buffer, and the cell lysis was conducted according to the vendor's protocol.

The Picogreen DNA quantification kit was used to quantify the DNA content of each sample following the manufacturer's instruction.[7] Alkaline phosphatase (ALP) activity was assessed by the hydrolysis of β-nitrophenyl phosphate as the substrate. Briefly, 20 μL of the cell lysates was mixed with 200 μL of ALP substrate and incubated for 1 h at 37 °C in the dark. Then, 10 μL of 0.02 M NaOH was added to stop the hydrolysis reaction. 220 μL of ALP substrate mixed with 10 μL of 0.02 M NaOH was used as a blank control. The absorbance was read at 405 nm and the ALP content was calculated from a standard calibration curve.

Osteocalcin Secretion. The osteocalcin secretion on day 14 and day 28 was measured using an intact human osteocalcin EIA kit BT-460 (Biomedical Technologies Inc., Stoughton, MA). The osteocalcin content was analyzed using the kit according to the manufacturer's instructions.[7]

Statistical Analysis. One-way ANOVA statistical analysis was performed to evaluate the significance of the experimental data. A p value of 0.05 was selected as the level of significance, and the data were indicated with (*) for $p < 0.05$, (**) for $p < 0.01$, and (***) for $p < 0.001$, respectively.

RESULTS AND DISCUSSION

Fabrication and Characterization of GO-Incorporated PLGA Nanofibrous Mats. PLGA nanofibrous mat was formed according to our previous work.[46] To obtain uniform PLGA and GO-incorporated PLGA nanofibrous mats, the concentrations of the PLGA solution was optimized to be in a range of 15−18%. In this work, the PLGA concentrations 15% and 18% were chosen for electrospinning.

The morphology of the formed nanofibrous mats was observed by SEM (Figure 1). It is clear that with or without GO, the PLGA nanofibrous mats display a porous 3D structure with a smooth surface, and the diameter of 15-PLGA nanofibers (concentration of PLGA solution for electrospinning is 15%) keeps a relatively narrow distribution range, with a mean

DOI: 10.1021/acsami.5b00862
ACS Appl. Mater. Interfaces 2015, 7, 6331−6339

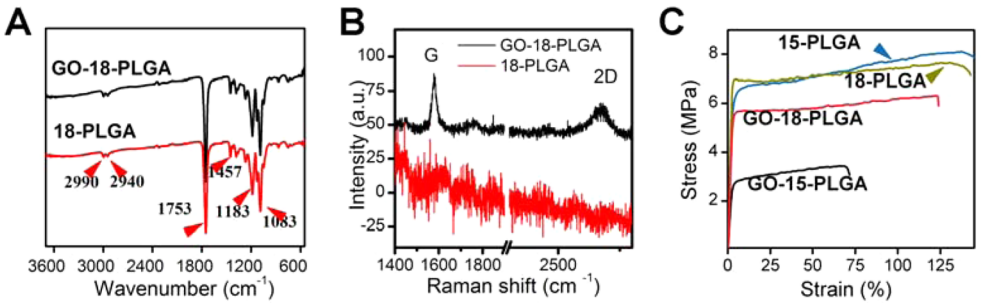

Figure 2. (A) FTIR spectra, (B) Raman spectra, and (C) representative stress−strain curves of PLGA nanofibrous mats and GO incorporated PLGA nanofibrous scaffolds, respectively.

diameter of 829 ± 146 nm. The mean diameter of 18-PLGA (concentration of PLGA solution for electrospinning is 18%) is 1461 ± 276 nm. After GO was added into the PLGA solution, the mean diameter of 15-PLGA nanofibers decreased from 829 to 783 nm, and the mean diameter of 18-PLGA nanofibers decreased from 1461 to 1222 nm. The decrease of fiber diameter is probably due to the change of electrospinning solution properties caused by the addition of GO.[46] The porous structure and the diameter of fibers are similar to the topological structure of natural ECM, and therefore well mimic the extracellular environment of cells, facilitating cell attachment and proliferation.[43] As shown in Figure 1, the nanofiber with smooth surface could not see GO on the surface of nanofiber. We speculate that the GO nanosheets might be embedded in the nanofibers and aligned along the axial direction of shape anisotropy of regular shapes in nanofibers similar to the literature reported by Lee and his co-workers.[47]

The PLGA and GO-incorporated PLGA nanofibrous mats were first characterized by attenuated total reflectance (ATR)-FTIR (Figure 2A). The characterized peaks, of PLGA around 2990 cm^{-1} and 2940 cm^{-1} were assigned to $-CH_2$, 1753 cm^{-1} was assigned to C═O, 1183 cm^{-1} and 1083 cm^{-1} were assigned to C—O), are clearly seen.[40] Compared with the PLGA nanofibers, the GO-doped PLGA nanofibrous mat exhibits no visible alteration in the FTIR spectra, suggesting that the GO dispersed into the electrospinning solution only by physical mixing, instead of chemical reaction. To confirm the mixture of GO in the PLGA nanofibers, Raman spectra were recorded. The Raman spectrum of GO-18-PLGA nanofibrous mat showed characteristic G band and 2D peak of GO at 1584 and 2682 cm^{-1}, respectively (Figure 2B),[48,49] clearly suggesting presence of GO in the GO-PLGA nanofibrous scaffolds.

For applications of GO-incorporated PLGA nanofibrous mats as tissue engineering scaffolds, several key factors, such as hydrophilicity, mechanical strength, and biocompatibility, have to be investigated. Water contact angle measurement showed that after GO was added, the contact angles of 15-PLGA and 18-PLGA nanofibrous mats decreased from 123 ± 4° to 115 ± 4°, and 122 ± 4° to 111 ± 4°, respectively (Figure S1, Supporting Information), suggesting that the hydrophilicity of PLGA nanofibrous mat increased slightly after mixing with GO. Besides the changes of surface hydrophilicity, the impact of the GO incorporation on the mechanical strength of the PLGA nanofibrous mat was probed. The strain−stress curves (Figure 2C) and the mechanical parameters of 15-PLGA, GO-15-PLGA, 18-PLGA, and GO-18-PLGA are listed in Table 1. It is clear that all the materials possess excellent mechanical properties. But the breaking strength and Young's modulus decrease after the addition of 1% GO. This can be explained as follows: due to its 2D topological plane structure, GO might tend to be vertical to the fibers. When the fibers are under stress, GO cannot transfer the part force, leading to the decrease of breaking strength.

Table 1. Mechanical Properties of Electrospun Nanofibrous Mats (15-PLGA, GO-15-PLGA, 18-PLGA, and GO-18-PLGA)

samples	tensile stress (MPa)	ultimate strain (%)	Young's modulus (MPa)
15-PLGA	5.8 ± 0.9	134.3 ± 4.4	106.4 ± 18.4
GO-15-PLGA	2.8 ± 0.3	66.9 ± 2.9	76.3 ± 9.4
18-PLGA	6.4 ± 0.5	133.6 ± 26.8	182.7 ± 8.00
GO-18-PLGA	5.7 ± 0.7	87.5 ± 8.5	134.4 ± 26.5

The data are expressed as mean ± SD, n = 3.

Protein Preconcentration onto the GO-Incorporated PLGA Nanofibrous Scaffolds. The adsorption of proteins onto the surface of substrates is an essential issue for regulating the cell functions, because they could directly mediate cell adhesion and morphology.[50,51] It has been found that 15-PLGA and 18-PLGA nanofibrous mats have similar protein adsorption behaviors. Encouragingly, GO-incorporated nanofibrous mats (GO-15-PLGA and GO-18-PLGA) were able to adsorb much more proteins (Figure 3A) than the corresponding mats without GO doping. Doping GO into PLGA nanofibrous scaffolds could significantly improve the loading capacity of proteins. It was reported that GO has remarkable capabilities of protein adsorption, such as cytochrome c, bovine serum albumin, ribonuclease A, and protein kinase A.[32,35] Our previous work also demonstrated that GO could load proteins with a high payload capacity.[32,52] Additionally, the hydrophilic nature of the GO-incorporated PLGA nanofibrous substrates is also likely responsible for the improved protein loading. The enrichment of proteins on the GO-incorporated PLGA nanofibrous scaffolds facilitates the hMSCs adhesion and proliferation.

The adsorption of GO-15-PLGA and GO-18-PLGA nanofibrous substrates toward cell growth and differentiation agents is one of the key factors that influence hMSCs growth and differentiation in our research. We found that the GO-incorporated PLGA nanofibrous scaffolds efficiently preconcentrated DEXA (Figure 3B), a classical osteogenic inducer during bone differentiation.[53] GO-15-PLGA and GO-18-PLGA nanofibrous mats adsorbed up to 45% and 44% of DEXA, respectively, compared to only less than 40% loading on the PLGA nanofibers. All the nanofibers could efficiently bind ascorbic acid (Figure 3C). The preconcentration effect of the

DOI: 10.1021/acsami.5b00862
ACS Appl. Mater. Interfaces 2015, 7, 6331−6339

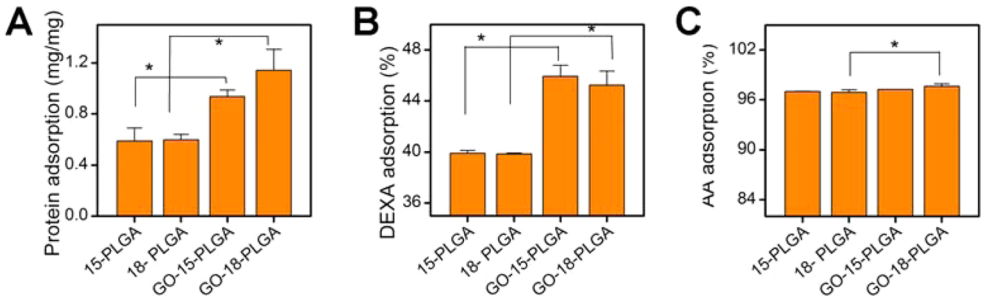

Figure 3. Adsorption profiles of (A) protein, (B) DEXA, and (C) ascorbic acid on the 15-PLGA, GO-15-PLGA, 18-PLGA, and GO-18-PLGA nanofibrous substrates, respectively. (* $p < 0.05$).

GO-incorporated PLGA nanofibrous mats might increase the concentration of the DEXA, AA and proteins onto the surface of the nanofibrous mats. Then, it could accelerate the exchange of inducer and nutrient substance between the hMSCs and the medium, which could regulate postdifferentiated, mature osteoblasts.[54]

Hemocompatibility of GO-Incorporated PLGA Nanofibrous Mats. Hemocompatibility of the scaffolds is a major concern when they are intended to contact blood in vivo. Hence, we investigated the hemocompatibility of the PLGA nanofibers with or without GO (Figure 4). No visible hemolytic

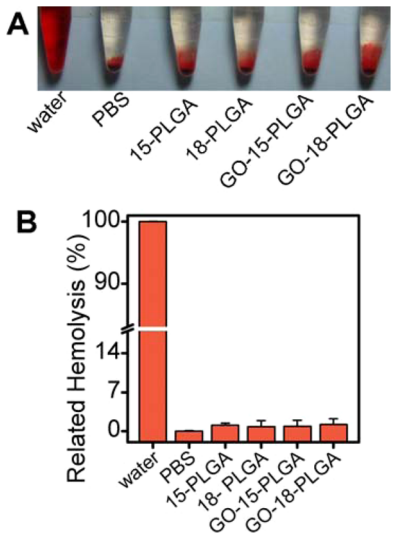

Figure 4. (A) Photo of solution of RBCs treated with different nanofibrous samples, followed by centrifugation. (B) Relative hemolysis of RBCs after being incubated with water, PBS, 15-PLGA, 18-PLGA, GO-15-PLGA, and GO-18-PLGA nanofibers, respectively.

phenomenon was observed when the RBC suspension was treated with fiber mats in vitro (Figure 4A). As shown in Figure4b, the relative hemolysis percentage of positive control (water) is 100%, whereas the negative control (PBS) is 0%. The relative hemolysis percentages of the PLGA or GO-incorporated PLGA nanofibrous mats were all less than 2%, suggesting that all the nanofibrous mats show excellent hemocompatibility (Figure 4B).

Cell Adhesion and Proliferation. The hMSCs attachment and proliferation were investigated to evaluate whether the GO-incorporated PLGA nanofibrous mats satisfied the fundamental requirement in skeletal tissue engineering, and how the added GO played a role in cellular metabolism. The attachment behavior of the hMSCs onto the nanofibers was evaluated in 8 h (Figure 5). Compared with the control group (TCP substrate), hMSCs exhibited good adhesion to the PLGA and

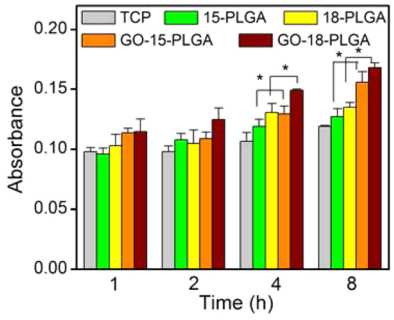

Figure 5. MTT assay of the adhesion viability of hMSCs seeded onto the PLGA and GO-incorporated PLGA fibrous mats, respectively. TCP was used as a control. (* $p < 0.05$).

the GO-incorporated PLGA nanofibers. The porous structure of electrospun nanofibrous mats and the protein loading capability of GO afford the scaffolds with a better attachment viability.[13]

Cell proliferation on the GO-incorporated PLGA nanofibers was also evaluated by MTT assay after 1, 3, and 7 d of culture. As shown in Figure 6A, the hMSCs cultured on the nanofibers grew better than those cultured on TCP on 3rd day, and especially on 7th day. There is a lag phase when seeding the hMSCs onto the nanofibrous scaffolds or TCP, giving rise to the slow cell proliferation. After GO was doped into the PLGA nanofibers, the rate of cell proliferation increased dramatically. This result is in agreement with previous literature.[35] The enhanced hMSCs growth is probably due to the adsorption of the protein to the GO-15-PLGA and GO-18-PLGA scaffolds.

The morphology of the hMSCs cells on the PLGA nanofibrous mats with or without doping GO after 28 d of incubation was examined by SEM (Figure 6B). The nanofibrous feature of the PLGA and the GO-incorporated PLGA substrates was well preserved after incubation for 28 d, and the cells spread and proliferated well on the nanofibrous mats. As shown in Figure 6B, we did not see more cells on the surface of nanofibrous mats, because hMSCs can penetrate into the scaffolds due to the 3D porous structure of the scaffolds, in agreement with the literature.[55]

Osteogenic Differentiation. MSCs can undergo osteogenic differentiation and form bone for regeneration. Specific markers were measured to determine the alteration of hMSCs into specific cell types.

Variations of marker genes of hMSCs and osteoblasts were quantitatively detected by RT-PCR. Quantitative analysis of

DOI: 10.1021/acsami.5b00862
ACS Appl. Mater. Interfaces 2015, 7, 6331−6339

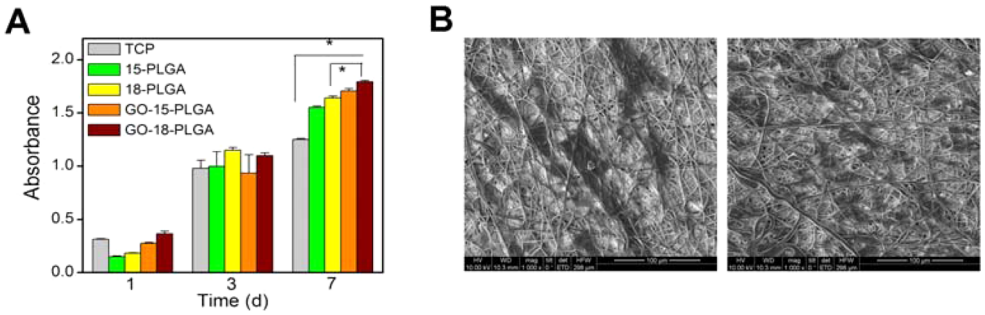

Figure 6. (A) MTT assay of the proliferation of mesenchymal stem cells seeded onto tissue culture plate and graphene oxide-incorporated PLGA scaffolds after 1, 3, and 7 d coculture. (* $p < 0.05$). (B) SEM images of the 18-PLGA (left) and GO-18-PLGA (right) nanofibrous mats cultured with hMSCs.

mRNA expression levels of CD44 and CD105 was first measured (Figure 7). With increasing incubation time, the

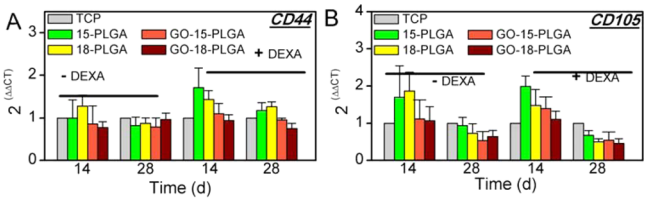

Figure 7. RT-PCR for variation of hMSC marker genes of (A) CD44 and (B) CD105 of hMSCs cultured onto the PLGA and GO-incorporated PLGA fibrous mats for 14 and 28 d, respectively. The hMSCs cultured onto TCP were taken as a control.

hMSC marker genes (CD44 and CD105) of cells cultured on the PLGA and GO-incorporated PLGA nanofibers decreased slightly. In differential medium with osteogenic inducer (DEXA), decreasing expression of CD44 and CD105 was obvious, likely due to the formation of bone at day 28.

ALP enzyme, an osteogenesis marker that often presents at high expression level in osteoblasts, is related to the early outset of mineralization of newly bone formation (Figure 8). In the medium supplemented with DEXA, the amount of ALP and collagen type I (Col I) extracted from the hMSCs cultured on GO-15-PLGA and GO-18-PLGA platforms was obviously higher than those cultured on 15-PLGA and 18-PLGA scaffolds ($p < 0.05$). Col I is another key marker for the bone formation process. These two osteogenic related genes represent nearly 2-fold increased expression in the hMSCs cultured on the GO incorporated PLGA substrates compared to those cultured on the PLGA substrates at day 14, and 3-fold to 5-fold increased expression at day 28. These facts indicated that adding GO to PLGA nanofibers accelerated stem cells differentiation. Additionally, another specific marker gene of osteogenic differentiation, osteocalcin (Ocn), which is a late stage osteogenesis and mineralization marker, was further evaluated to figure out the stem cell phenotype. With increasing incubation time, the expression level of Ocn gene was enhanced, suggesting osteogenic differentiation of hMSCs on the nanofibrous platforms. Similar to ALP and Col I, in the presence of DEXA, the expression levels of Ocn gene of hMSCs cultured on the GO-doped nanofibers were significantly high, compared to those on the PLGA nanofibers (Figure 8).

The ALP activity of hMSCs was examined on day 14 and on day 28, and the results (normalized for the total DNA content) are shown in Figure 9A. It is clear that from day 14 to day 28, hMSCs on 15-PLGA and 18-PLGA nanofibers in differentiation

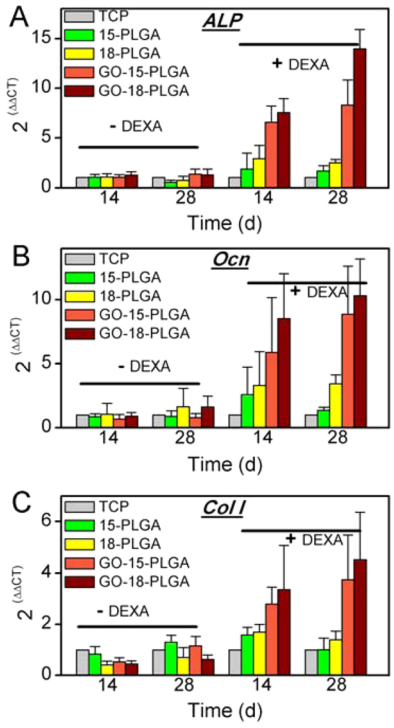

Figure 8. RT-PCR for variation of osteoblasts marker genes of (A) ALP, (B) Ocn, and (C) Col I after hMSCs seeded onto the PLGA and GO-incorporated PLGA fibrous mats with or without DEXA, for 14 and 28 d, respectively.

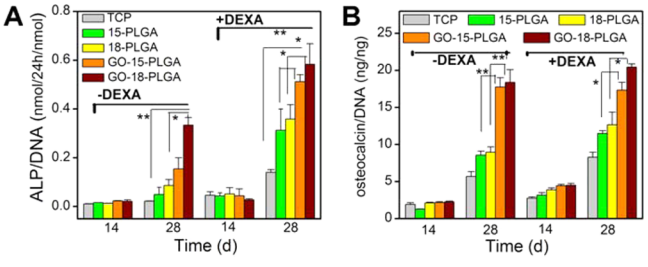

Figure 9. (A) ALP activity (normalized for the DNA content, *n* mol of transformed substrate per unit of time and per mass of DNA) of hMSCs seeded on different substrates (TCP, 15-PLGA, 18-PLGA, GO-15-PLGA, and GO-18-PLGA) after 14 and 28 d of coculture, with or without osteogenic inducer, respectively. (B) Osteocalcin secretion of hMSCs cultured onto TCP, 15-PLGA, 18-PLGA, GO-15-PLGA, and GO-18-PLGA platforms with or without DEXA in the culture medium, for 14 and 28 d, respectively. (* $p < 0.05$, ** $p < 0.01$).

DOI: 10.1021/acsami.5b00862
ACS Appl. Mater. Interfaces 2015, 7, 6331−6339

medium displayed a gradual enhancement of osteogenic differentiation. As expected, hMSCs seeded on the GO-incorporated PLGA nanofibrous scaffolds showed significantly higher ALP activity than those on the PLGA nanofibers and TCP in differentiation medium, even without DEXA. After 14 d, ALP activity of hMSCs in all experimental groups was found to be at low level, likely due to the fact that the hMSCs are in the proliferation phase, consistent with RT-PCR analysis of hMSCs marker genes. After 28 d of incubation, hMSCs cultured onto the GO-incorporated PLGA nanofibers had significantly increased ALP activity. It should be pointed out that under DEXA induction, hMSCs cultured on GO-15-PLGA and GO-18-PLGA platforms were more osteogenic than other substrates used.

The extracellular osteocalcin contents produced by the hMSCs on TCP, PLGA and GO-PLGA nanofibers were also measured after culturing for 14 and 28 d, respectively (Figure 9B). On day 14, the hMSCs incubated in both growth medium and differential medium generated very low levels of osteocalcin contents. However, the hMSCs cultured in both medium (with or without DEXA) for 28 d generated much higher levels of osteocalcin content than those cultured for 14 d, reflecting the progression of osteogenic differentiation. In addition, the GO-15-PLGA and GO-18-PLGA groups had much high osteocalcin production than the 15-PLGA and 18-PLGA nanofibers groups, respectively ($p < 0.01$), demonstrating the effect of GO doping within the PLGA nanofibers on the enhancement of osteogenic differentiation. In differentiation medium (with DEXA), the hMSCs on TCP substrate secreted much more osteocalcin than those treated in the absence of DEXA, indicating induction of osteogenesis of hMSCs by adding DEXA. PLGA and the GO-doped PLGA groups displayed significantly high levels of osteocalcin secretion, compared with the TCP group, which may be relevant to the 3D structure of the nanofibers, inducing differentiation by forcing the cells into an osteogenic morphology, as previously reported.[56] The cells cultured on both the PLGA nanofibers and the GO-incorporated PLGA nanofibers secreted much more osteocalcin than those on the TCP substrate, similar to the RT-PCR and ALP activity results discussed above. Overall, the evaluation of the late-stage differentiation marker suggests that the GO-PLGA nanofibers are suitable scaffold for osteogenic differentiation of hMSCs, even in the absence of osteogenic supplements.

The above results suggested that hMSCs cultured on the GO-incorporated PLGA nanofibrious mats were more osteogenic, especially under DEXA induction, than those on the PLGA nanofibrious mats and TCP. The GO-incorporated PLGA nanofibrious mats could efficiently preconcentrate proteins and DEXA, which benefits cell growth and mineral deposition of hMSCs.[57] The enhancement of attachment, growth and osteogenic differentiation of hMSCs on GO-15-PLGA and GO-18-PLGA substrates is probably due to the following reasons: First, the porous structure of the nanofibrous mats endows ECM biomimetic microenvironment for hMSCs adhesion and proliferation. Second, GO increased local concentration of proteins and osteogenic inducer on the surface of the scaffolds (GO-15-PLGA and GO-18-PLGA). Lee et al. reported that CVD grown graphene and GO substrates were able to preconcentrate DEXA and β-GP via physical interactions.[35] They also found that CVD grown graphene and GO substrates could promote differentiation of MSCs toward osteogenic differentiation.

In addition to the chemical inducer for hMSCs differentiation, the mechanical properties of the platforms may involve in hMSCs metabolism. Stiff substrates with appropriate physical stress (>100 kPa) promote osteogenic differentiation.[40] The PLGA nanofibers with or without GO doping exhibited the Young's modulus in the range of 70 to 180 MPa. However, the Young's modulus of GO-15-PLGA and GO-18-PLGA nanofibrous mats were decreased after GO adding. The decreased mechanical stress was unlikely to regulate the osteogenic specification. Actually, the preconcentration capability of proteins and DEXA by GO and GO-incorporated PLGA platforms may be mainly responsible for the enhancement of hMSCs bone differentiation in the current work. Thus, GO-doped PLGA platforms may find potential applications as biodegradable substrates for bone regeneration.

CONCLUSIONS

In summary, the GO-incorporated PLGA nanofibrious mats were fabricated via an electrospinning approach and explored for using as scaffold materials for tissue engineering. GO can be readily electrospun into PLGA nanofibers without changing the 3D porous structure. Doping of GO into nanofibrious mats leads to slightly increase in the hydrophilicity, and significant improvement in the adsorption ability and preconcentration capacity. The GO-doped PLGA nanofibrous mats afford ECM biomimetic microenvironment for hMSCs adhesion and proliferation. Thus, the GO-incorporated PLGA nanofibers could serve as novel tissue engineering scaffolds with good biocompatibility. Our results demonstrated that the GO-doped PLGA substrate induces expression of osteogenic marker genes such as ALP, Col I, and Ocn. Meanwhile, it promotes ALP activity and osteocalcin secretion. The PLGA nanofibers incorporated with GO not only promote the attachment and proliferation of hMSCs but also enhance the hMSCs differentiation toward osteoblast, which is important for biomedical applications requiring the biomimetic of ECM. Taking together, this work provides a convenient, simple and powerful approach to the formation of GO-incorporated PLGA nanofibers for potential applications in tissue engineering and other biomedical fields.

ASSOCIATED CONTENT

Supporting Information

Contact angle of electrospun nanofibrous mats, the DNA content and the primers for RT-PCR. This material is available free of charge via the Internet at http://pubs.acs.org/.

AUTHOR INFORMATION

Corresponding Authors

*J. Dai. E-mail: jwdai@genetics.ac.cn. Tel.: +86-10-82614426.
*X. Shi. E-mail: xshi@dhu.edu.cn. Tel.: +86-21-67792656.
*Z. Zhang. E-mail: zjzhang2007@sinano.ac.cn. Tel.: +86-512-62872556.

Author Contributions

$^{\perp}$These authors contributed equally to this work. The paper was written through contributions of all authors. All authors have given approval to the final version of the paper.

Notes

The authors declare no competing financial interest.

DOI: 10.1021/acsami.5b00862
ACS Appl. Mater. Interfaces 2015, 7, 6331−6339

■ ACKNOWLEDGMENTS

We acknowledge financial support of this work from National Natural Science Foundation of China (No. 51361130033) and the Ministry of Science and Technology of China (No. 2014CB965003). X. Shi thanks the Program for Professor of Special Appointment (Eastern Scholar) at Shanghai Institutions of Higher Learning. We also thank Professor Wei Chen at SINANO for assistance with the electrospinning facility.

■ REFERENCES

(1) Mei, F.; Zhong, J. S.; Yang, X. P.; Ouyang, X. Y.; Zhang, S.; Hu, X. Y.; Ma, Q.; Lu, J. G.; Ryu, S. K.; Deng, X. L. Improved Biological Characteristics of Poly(L-lactic acid) Electrospun Membrane by Incorporation of Multiwalled Carbon Nanotubes/Hydroxyapatite Nanoparticles. *Biomacromolecules* **2007**, *8*, 3729−3735.

(2) Ionescu, L. C.; Lee, G. C.; Sennett, B. J.; Burdick, J. A.; Mauck, R. L. An Anisotropic Nanofiber/Microsphere Composite with Controlled Release of Biomolecules for Fibrous Tissue Engineering. *Biomaterials* **2010**, *31*, 4113−4120.

(3) Xiao, S.; Shen, M.; Guo, R.; Wang, S.; Shi, X. Immobilization of Zerovalent Iron Nanoparticles into Electrospun Polymer Nanofibers: Synthesis, Characterization, and Potential Environmental Applications. *J. Phys. Chem. C* **2009**, *113*, 18062−18068.

(4) Huang, Y.; Ma, H.; Wang, S.; Shen, M.; Guo, R.; Cao, X.; Zhu, M.; Shi, X. Efficient Catalytic Reduction of Hexavalent Chromium Using Palladium Nanoparticle-Immobilized Electrospun Polymer Nanofibers. *ACS Appl. Mater. Interfaces* **2012**, *4*, 3054−3061.

(5) Fang, X.; Ma, H.; Xiao, S.; Shen, M.; Guo, R.; Cao, X.; Shi, X. Facile Immobilization of Gold Nanoparticles into Electrospun Polyethyleneimine/Polyvinyl Alcohol Nanofibers for Catalytic Applications. *J. Mater. Chem.* **2011**, *21*, 4493−4501.

(6) Ruiling, Q.; Huijuan, L. Electrospun MWCNTs/Poly(lactic-co-glycolic acid) Composite Nanofibrous Drug Delivery System. *Adv. Mater. Res.* **2012**, *424*−*425*, 1220−1223.

(7) Wang, S. G.; Castro, R.; An, X.; Song, C. l.; Luo, Y.; Shen, M. W.; Tomas, H.; Zhu, M. F.; Shi, X. Y. Electrospun Laponite-Doped Poly(lactic-co-glycolic acid) Nanofibers for Osteogenic Differentiation of Human Mesenchymal Stem Cells. *J. Mater. Chem.* **2012**, *22*, 23357−23367.

(8) Qi, R.; Guo, R.; Shen, M.; Cao, X.; Zhang, L.; Xu, J.; Yu, J.; Shi, X. Electrospun Poly (lactic-co-glycolic acid)/Halloysite Nanotube Composite Nanofibers for Drug Encapsulation and Sustained Release. *J. Mater. Chem.* **2010**, *20*, 10622−10629.

(9) Meng, J.; Xiao, B.; Zhang, Y.; Liu, J.; Xue, H.; Lei, J.; Kong, H.; Huang, Y.; Jin, Z.; Gu, N.; Xu, H. Super-Paramagnetic Responsive Nanofibrous Scaffolds under Static Magnetic Field Enhance Osteogenesis for Bone Repair in Vivo. *Sci. Rep.* **2013**, *3*, 1−7.

(10) Harrington, D. A.; Cheng, E. Y.; Guler, M. O.; Lee, L. K.; Donovan, J. L.; Claussen, R. C.; Stupp, S. I. Branched Peptide-Amphiphiles as Self-Assembling Coatings for Tissue Engineering Scaffolds. *J. Biomed. Mater. Res., Part A* **2006**, *78A*, 157−167.

(11) Yoshimoto, H.; Shin, Y. M.; Terai, H.; Vacanti, J. P. A Biodegradable Nanofiber Scaffold by Electrospinning and Its Potential for Bone Tissue Engineering. *Biomaterials* **2003**, *24*, 2077−2082.

(12) Abraham, S.; Riggs, M. J.; Nelson, K.; Lee, V.; Rao, R. R. Characterization of Human Fibroblast-Derived Extracellular Matrix Components for Human Pluripotent Stem Cell Propagation. *Acta Biomater.* **2010**, *6*, 4622−4633.

(13) Sottile, J. Regulation of Angiogenesis by Extracellular Matrix. *Biochim. Biophys. Acta, Rev. Cancer* **2004**, *1654*, 13−22.

(14) Wei, G. B.; Ma, P. X. Nanostructured Biomaterials for Regeneration. *Adv. Funct. Mater.* **2008**, *18*, 3568−3582.

(15) Reneker, D. H.; Chun, I. Nanometre Diameter Fibres of Polymer, Produced by Electrospinning. *Nanotechnology* **1996**, *7*, 216−223.

(16) Huang, C.; Chen, R.; Ke, Q. F.; Morsi, Y.; Zhang, K. H.; Mo, X. M. Electrospun Collagen-Chitosan-TPU Nanofibrous Scaffolds for Tissue Engineered Tubular Grafts. *Colloids Surf., B Biointerfaces* **2011**, *82*, 307−315.

(17) Bhattarai, N.; Li, Z. S.; Edmondson, D.; Zhang, M. Q. Alginate-based Nanofibrous Scaffolds: Structural, Mechanical, and Biological Properties. *Adv. Mater.* **2006**, *18*, 1463−1467.

(18) Li, W. J.; Laurencin, C. T.; Caterson, E. J.; Tuan, R. S.; Ko, F. K. Electrospun Nanofibrous Structure: A Novel Scaffold for Tissue Engineering. *J. Biomed. Mater. Res.* **2002**, *60*, 613−621.

(19) Mo, X. M.; Xu, C. Y.; Kotaki, M.; Ramakrishna, S. Electrospun P(LLA-CL) Nanofiber: A Biomimetic Extracellular Matrix for Smooth Muscle Cell and Endothelial Cell Proliferation. *Biomaterials* **2004**, *25*, 1883−1890.

(20) Shin, M.; Yoshimoto, H.; Vacanti, J. P. In Vivo Bone Tissue Engineering Using Mesenchymal Stem Cells on a Novel Electrospun Nanofibrous Scaffold. *Tissue Eng.* **2004**, *10*, 33−41.

(21) Ebrahimi-Barough, S.; Javidan, A. N.; Saberi, H.; Joghataei, M. T.; Rahbarghazi, R.; Mirzaei, E.; Faghihi, F.; Shirian, S.; Ai, A.; Ai, J. Evaluation of Motor Neuron-like Cell Differentiation of hEnSCs on Biodegradable PLGA Nanofiber Scaffolds. *Mol. Neurobiol.* **2014**, DOI: 10.1007/s12035-014-8931-2.

(22) Wang, J.; Cui, X.; Zhou, Y.; Xiang, Q. Core-Shell PLGA/Collagen Nanofibers Loaded with Recombinant FN/CDHs as Bone Tissue Engineering Scaffolds. *Connect. Tissue Res.* **2014**, *55*, 292−298.

(23) Meng, Z.; Li, H.; Sun, Z.; Zheng, W.; Zheng, Y. Fabrication of Mineralized Electrospun PLGA and PLGA/Gelatin Nanofibers and Their Potential in Bone Tissue Engineering. *Mater. Sci. Eng., C* **2013**, *33*, 699−706.

(24) Soscia, D. A.; Sequeira, S. J.; Schramm, R. A.; Jayarathanam, K.; Cantara, S. I.; Larsen, M.; Castracane, J. Salivary Gland Cell Differentiation and Organization on Micropatterned PLGA Nanofiber Craters. *Biomaterials* **2013**, *34*, 6773−6784.

(25) Haider, A.; Gupta, K. C.; Kang, I. K. PLGA/nHA Hybrid Nanofiber Scaffold as a Nanocargo Carrier of Insulin for Accelerating Bone Tissue Regeneration. *Nanoscale Res. Lett.* **2014**, *9*, 1−12.

(26) Caballero, M.; Skancke, M. D.; Halevi, A. E.; Pegna, G.; Pappa, A. K.; Krochmal, D. J.; Morse, J.; van Aalst, J. A. Effects of Connective Tissue Growth Factor on the Regulation of Elastogenesis in Human Umbilical Cord-Derived Mesenchymal Stem Cells. *Ann. Plast. Surg.* **2013**, *70*, 568−573.

(27) Loh, K. P.; Bao, Q. L.; Eda, G.; Chhowalla, M. Graphene Oxide as a Chemically Tunable Platform for Optical Applications. *Nat. Chem.* **2010**, *2*, 1015−1024.

(28) Liu, G. D.; Shen, H.; Mao, J. N.; Zhang, L. M.; Jiang, Z.; Sun, T.; Lan, Q.; Zhang, Z. J. Transferrin Modified Graphene Oxide for Glioma-Targeted Drug Delivery: In Vitro and in Vivo Evaluations. *ACS Appl. Mater. Interfaces* **2013**, *5*, 6909−6914.

(29) Zhang, L. M.; Xia, J. H.; Zhao, Q. H.; Liu, L. W.; Zhang, Z. J. Functional Graphene Oxide as a Nanocarrier for Controlled Loading and Targeted Delivery of Mixed Anticancer Drugs. *Small* **2010**, *6*, 537−544.

(30) Zhang, L. M.; Wang, Z. L.; Lu, Z. X.; Shen, H.; Huang, J.; Zhao, Q. H.; Liu, M.; He, N. Y.; Zhang, Z. J. PEGylated Reduced Graphene Oxide as a Superior ssRNA Delivery System. *J. Mater. Chem. B* **2013**, *1*, 749−755.

(31) Zhang, L. M.; Lu, Z. X.; Zhao, Q. H.; Huang, J.; Shen, H.; Zhang, Z. J. Enhanced Chemotherapy Efficacy by Sequential Delivery of siRNA and Anticancer Drugs Using PEI-Grafted Graphene Oxide. *Small* **2011**, *7*, 460−464.

(32) Shen, H.; Liu, M.; He, H. X.; Zhang, L. M.; Huang, J.; Chong, Y.; Dai, J. W.; Zhang, Z. J. PEGylated Graphene Oxide-Mediated Protein Delivery for Cell Function Regulation. *ACS Appl. Mater. Interfaces* **2012**, *4*, 6317−6323.

(33) Lee, D. Y.; Khatun, Z.; Lee, J. H.; Lee, Y. K.; In, I. Blood Compatible Graphene/Heparin Conjugate through Noncovalent Chemistry. *Biomacromolecules* **2011**, *12*, 336−341.

(34) Kotchey, G. P.; Allen, B. L.; Vedala, H.; Yanamala, N.; Kapralov, A. A.; Tyurina, Y. Y.; Klein-Seetharaman, J.; Kagan, V. E.; Star, A. The Enzymatic Oxidation of Graphene Oxide. *ACS Nano* **2011**, *5*, 2098−2108.

DOI: 10.1021/acsami.5b00862
ACS Appl. Mater. Interfaces 2015, 7, 6331−6339

(35) Lee, W. C.; Lim, C. H. Y. X.; Shi, H.; Tang, L. A. L.; Wang, Y.; Lim, C. T.; Loh, K. P. Origin of Enhanced Stem Cell Growth and Differentiation on Graphene and Graphene Oxide. *ACS Nano* **2011**, *5*, 7334−7341.
(36) Akhavan, O.; Ghaderi, E.; Shahsavar, M. Graphene Nanogrids for Selective and Fast Osteogenic Differentiation of Human Mesenchymal Stem Cells. *Carbon* **2013**, *59*, 200−211.
(37) Nayak, T. R.; Andersen, H.; Makam, V. S.; Khaw, C.; Bae, S.; Xu, X. F.; Ee, P. L. R.; Ahn, J. H.; Hong, B. H.; Pastorin, G.; Oezyilmaz, B. Graphene for Controlled and Accelerated Osteogenic Differentiation of Human Mesenchymal Stem Cells. *ACS Nano* **2011**, *5*, 4670−4678.
(38) Ku, S. H.; Park, C. B. Myoblast Differentiation on Graphene Oxide. *Biomaterials* **2013**, *34*, 2017−2023.
(39) Xin, X. J.; Hussain, M.; Mao, J. J. Continuing Differentiation of Human Mesenchymal Stem Cells and Induced Chondrogenic and Osteogenic Lineages in Electrospun PLGA Nanofiber Scaffold. *Biomaterials* **2007**, *28*, 316−325.
(40) Engler, A. J.; Sen, S.; Sweeney, H. L.; Discher, D. E. Matrix Elasticity Directs Stem Cell Lineage Specification. *Cell* **2006**, *126*, 677−689.
(41) Dalby, M. J.; Gadegaard, N.; Tare, R.; Andar, A.; Riehle, M. O.; Herzyk, P.; Wilkinson, C. D. W.; Oreffo, R. O. C. The Control of Human Mesenchymal Cell Differentiation Using Nanoscale Symmetry and Disorder. *Nat. Mater.* **2007**, *6*, 997−1003.
(42) Liu, Z.; Robinson, J. T.; Sun, X. M.; Dai, H. J. PEGylated Nanographene Oxide for Delivery of Water-Insoluble Cancer Drugs. *J. Am. Chem. Soc.* **2008**, *130*, 10876−10877.
(43) Luo, Y.; Wang, S. G.; Shen, M. W.; Qi, R. L.; Fang, Y.; Guo, R.; Cai, H. D.; Cao, X. Y.; Tomas, H.; Zhu, M. F.; Shi, X. Y. Carbon Nanotube-Incorporated Multilayered Cellulose Acetate Nanofibers for Tissue Engineering Applications. *Carbohydr. Polym.* **2013**, *91*, 419−427.
(44) Meng, J.; Han, Z. Z.; Kong, H.; Qi, X. J.; Wang, C. Y.; Xie, S. S.; Xu, H. Y. Electrospun Aligned Nanofibrous Composite of MWCNT/Polyurethane to Enhance Vascular Endothelium Cells Proliferation and Function. *J. Biomed. Mater. Res., Part A* **2010**, *95A*, 312−320.
(45) Han, S.; Zhao, Y.; Xiao, Z.; Han, J.; Chen, B.; Chen, L.; Dai, J. W. The Three-Dimensional Collagen Scaffold Improves the Stemness of Rat Bone Marrow Mesenchymal Stem Cells. *J. Genet. Genomics* **2012**, *39*, 633−641.
(46) Qi, R. L.; Cao, X. Y.; Shen, M. W.; Guo, R.; Yu, J. Y.; Shi, X. Y. Biocompatibility of Electrospun Halloysite Nanotube-Doped Poly(lactic-co-glycolic acid) Composite Nanofibers. *J. Biomater. Sci., Polym. Ed.* **2012**, *23*, 299−313.
(47) Yoon, O. J.; Jung, C. Y.; Sohn, I. Y.; Kim, H. J.; Hong, B.; Jhon, M. S.; Lee, N. E. Nanocomposite Nanofibers of Poly(D,L-lactic-co-glycolic acid) and Graphene Oxide Nanosheets. *Compos., Part A* **2011**, *42*, 1978−1984.
(48) Kudin, K. N.; Ozbas, B.; Schniepp, H. C.; Prud'homme, R. K.; Aksay, I. A.; Car, R. Raman Spectra of Graphite Oxide and Functionalized Graphene Sheets. *Nano Lett.* **2008**, *8*, 36−41.
(49) Kim, K. S.; Zhao, Y.; Jang, H.; Lee, S. Y.; Kim, J. M.; Kim, K. S.; Ahn, J.-H.; Kim, P.; Choi, J.-Y.; Hong, B. H. Large-Scale Pattern Growth of Graphene Films for Stretchable Transparent Electrodes. *Nature* **2009**, *457*, 706−710.
(50) Woo, K. M.; Seo, J.; Zhang, R. Y.; Ma, P. X. Suppression of Apoptosis by Enhanced Protein Adsorption on Polymer/Hydroxyapatite Composite Scaffolds. *Biomaterials* **2007**, *28*, 2622−2630.
(51) Woo, K. M.; Chen, V. J.; Ma, P. X. Nano-Fibrous Scaffolding Architecture Selectively Enhances Protein Adsorption Contributing to Cell Attachment. *J. Biomed. Mater. Res., Part A* **2003**, *67A*, 531−537.
(52) Cao, Y. H.; Chong, Y.; Shen, H.; Zhang, M. X.; Huang, J.; Zhu, Y. M.; Zhang, Z. J. Combination of TNF-Alpha and Graphene Oxide-Loaded BEZ235 to Enhance Apoptosis of PIK3CA Mutant Colorectal Cancer Cells. *J. Mater. Chem. B* **2013**, *1*, 5602−5610.
(53) Haynesworth, S. E.; Goshima, J.; Goldberg, V. M.; Caplan, A. I. Characterization of Cells with Osteogenic Potential from Human Marrow. *Bone* **1992**, *13*, 81−88.
(54) Quarles, L. D.; Yohay, D. A.; Lever, L. W.; Caton, R.; Wenstrup, R. J. Distinct Proliferative and Differentiated Stages of Murine MC3t3-E1 Cells in Culture - An in Vitro Model of Osteoblast Development. *J. Bone Miner. Res.* **1992**, *7*, 683−692.
(55) Liu, F.; Guo, R.; Shen, M.; Cao, X.; Mo, X.; Wang, S.; Shi, X. Effect of the Porous Microstructures of Poly(lactic-co-glycolic acid)/Carbon Nanotube Composites on the Growth of Fibroblast Cells. *Soft Mater.* **2010**, *8*, 239−253.
(56) Kumar, G.; Tison, C. K.; Chatterjee, K.; Pine, P. S.; McDaniel, J. H.; Salit, M. L.; Young, M. F.; Simon, C. G., Jr. The Determination of Stem Cell Fate by 3D Scaffold Structures through the Control of Cell Shape. *Biomaterials* **2011**, *32*, 9188−9196.
(57) Jaiswal, N.; Haynesworth, S. E.; Caplan, A. I.; Bruder, S. P. Osteogenic Differentiation of Purified, Culture-Expanded Human Mesenchymal Stem Cells in Vitro. *J. Cell. Biochem.* **1997**, *64*, 295−312.

DOI: 10.1021/acsami.5b00862
ACS Appl. Mater. Interfaces 2015, 7, 6331−6339